23P007-O

Model Analysis of Nanoscale Surface Roughness and Rippling during Plasma Etching of Si under Oblique Ion Incidence

プラズマエッチング時における表面ラフネス形成メカニズムとイオン入射角度依存性

Hirotaka Tsuda, Yoshinori Takao, Koji Eriguchi and Kouichi Ono
津田博隆，鷹尾祥典，江利口浩二，斧　高一

Department of Aeronautics and Astronautics, Graduate School of Engineering, Kyoto University, Yoshida-Honmachi, Sakyo-ku, Kyoto 606-8501, Japan
京都大学大学院工学研究科　航空宇宙工学専攻 〒606-8501　京都市左京区吉田本町

Three-dimensional atomic-scale cellular model has been developed to reproduce the formation of nanoscale or atomic-scale surface ripples during Si etching in chlorine-based plasmas under oblique ion incidence. Numerical results implied that ion incident angle and energy, and neutral-to-ion flux ratios play an important role in the formation of surface rippling or groove-like surface roughness.

1. Introduction

Three-dimensional measurement and prediction of atomic-scale surface roughness on etched features become increasingly important for the analysis of line edge roughness (LER) and line width roughness (LWR) on feature sidewalls during etching; however, the feature profiles are too small and/or too complex to measure the surface roughness on bottom surfaces and sidewalls of the etched features. To predict the surface roughness on atomic/nanometer scale, we have developed our own three-dimensional atomic-scale cellular model (ASCeM-3D) [1] and feature profile simulation. In this study, emphasis is placed on a better understanding of the formation mechanisms of atomic-scale surface roughness during Si etching in chlorine-based plasmas and the relationship between plasma parameters (ion incident angle, ion incident energy, and neutral-to-ion flux ratio) and etched feature profiles, with further attention being given to the formation of ripple structures on etched surfaces.

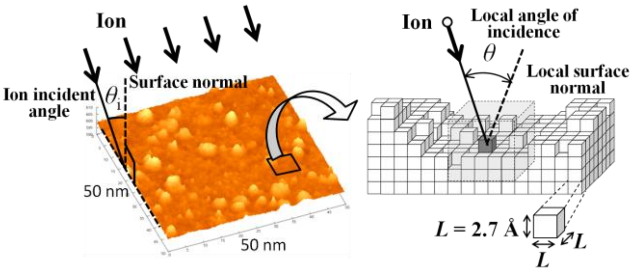

Fig. 1 Schematic of the ASCeM-3D model.

2. Modeling

In the ASCeM-3D model shown in Fig. 1, the simulation domain including substrates is divided into a number of small cubic cells of $L = \rho_{Si}^{-1/3}$ = 2.7 Å, where ρ_{Si} = 5.0 × 10^{22} cm^{-3} is the atomic density of Si substrates. Ions and neutrals are injected from the top of the simulation domain with a given incident angle θ_i and an isotropic distribution, respectively, and etch and/or sputter products are taken to be desorbed from etching surfaces into microstructural features thermally or isotropically with a cosine distribution. The particle transport is analyzed using the three-dimensional Monte Carlo (MC) algorithm, and the local surface normal or local angle θ of incidence is calculated by using the four-point technique for 5 × 5 × 5 neighboring cells (125 cells in total) at around the substrate surface cell that the ion reaches from the plasma. Two-body elastic collision processes between incident ions and substrate atoms are also taken into account to analyze the ion reflection on etched feature surfaces and penetration into substrates. The ASCeM-3D takes into account surface chemistries based on the MC algorithm [2-4], including adsorption and reemission of neutrals, chemical etching, ion-enhanced etching, physical sputtering, and redeposition of etch and/or sputter products on feature surfaces.

3. Results and Discussion

Figure 2 shows etch rates or *ER*s and roughness parameters (*RMS*) as a function of ion incident angle θ_i, simulated for different incident ion energies of E_i = 20, 50, 100, and 200 eV with an ion flux Γ_i^0 = 1.0 × 10^{16} $cm^{-2}s^{-1}$ and a neutral-to-ion flux ratio Γ_n^0/Γ_i^0 = 100, which are typical of high-density plasma etching environments. Numerical results indicated that *ER*s increase with increasing E_i and surface roughness becomes larger

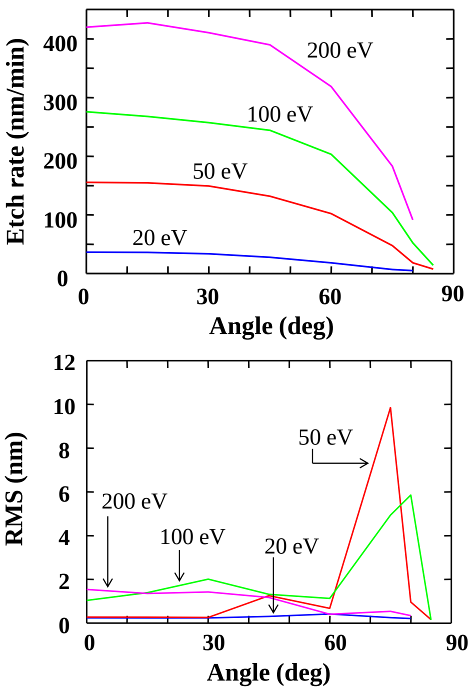

Fig. 2 Etch rates and roughness parameters (RMS) as a function of ion incident angle θ_i, simulated for different ion incident energies of E_i = 20, 50, 100, and 200 eV with a neutral-to-ion flux ratio Γ_n^0/Γ_i^0 = 100. Here, RMS is the root mean square roughness.

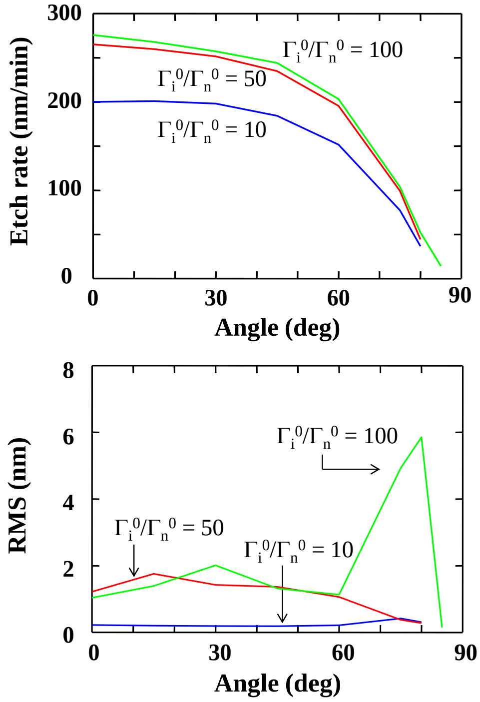

Fig. 3 Etch rates and roughness parameters (RMS) as a function of ion incident angle θ_i, simulated for different neutral-to-ion flux ratios of Γ_n^0/Γ_i^0 = 10, 50, and 100 with an ion incident energy E_i = 100. Here, RMS is the root mean square roughness.

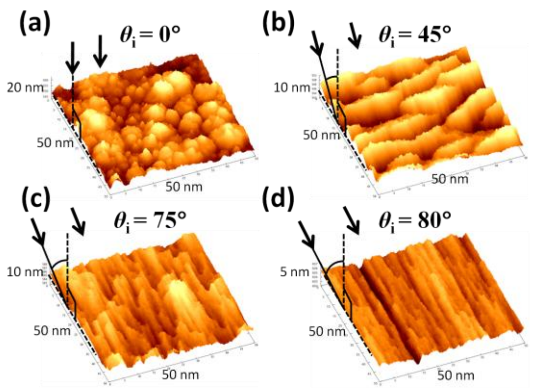

Fig. 4 Surface features of Si at t = 20 s after the start of etching in Cl_2 plasma, simulated for different ion incident angles of θ_i = (a) 0°, (b) 45°, (c) 75°, and (d) 80° with an ion energy E_i = 100 eV and neutral-to-ion flux ratios Γ_n^0/Γ_i^0 = 100.

at higher E_i for θ_i = 0° or normal incidence of ions. In addition, for increased θ_i or oblique ion incidence, surface roughness at E_i = 50 and 100 eV tends to become larger than that at higher E_i (= 200 eV).

In contrast, Fig. 4 shows *ER*s and the values of *RMS* as a function of ion incident angle θ_i, simulated for different neutral-to-ion flux ratios of Γ_n^0/Γ_i^0 = 10, 50, and 100 with E_i = 100. The comparison between the results in Fig. 3 and 4 indicates that there are different formation mechanisms between normal and oblique ion incidences, and ion incidence angle θ_i, ion incident energy E_i, and neutral-to-ion flux ratio Γ_n^0/Γ_i^0 play an important role in the roughness formation.

Figure 4 shows the surface features of Si at t = 20 s after the start of etching in Cl_2 plasma for different ion incident angles of θ_i = 0°, 45°, 75°, and 80°, simulated with E_i = 100 eV and Γ_n^0/Γ_i^0 = 100. Numerical results indicated that as the angle θ_i is increased, nanoscale convex features drastically change and the ripple structures of etched surfaces occur. For θ_i = 0° or normal incidence of ions, the surfaces are randomly roughened. For increased θ_i = 45°, the ripples are formed perpendicular to the direction of ion incidence, while parallel to that of ion incidence for further increased θ_i = 75° and 80°.

The ASCeM-3D model implied that neutral-to-ion flux ratio or the neutral particle supply to etched surfaces plays a role in the formation of surface rippling or groove-like surface roughness as important as ion incident angle and energy.

References

[1] H. Tsuda, H. Miyata, Y. Takao, K. Eriguchi, and K. Ono: Jpn. J. Appl. Phys. **50** (2011) 08JE06.

[2] Y. Osano, and K. Ono: J. Vac. Sci. Technol. B **26** (2008) 1425.

[3] H. Tsuda, M. Mori, Y. Takao, K. Eriguchi, and K. Ono: Thin Solid Films **518** (2010) 3475.

[4] H. Tsuda, M. Mori, Y. Takao, K. Eriguchi, and K. Ono: Jpn. J. Appl. Phys. **49** (2010) 08JE01.